Single Ca^+ Ion Trapping toward Precise Frequency Measurement of the 4 $^2S_{1/2}$ – 3 $^2D_{5/2}$ Transition

K. Matsubara, Y. Li, M. Kajita, K. Hayasaka, and M. Hosokawa
National Institute of Information and Communications Technology
Koganei, Tokyo, Japan
matubara@nict.go.jp

S. Urabe
Graduate School of Engineering Science
Osaka University
Toyonaka, Osaka, Japan

***Abstract*—We are proceeding with a development of an optical frequency standard using a $^2S_{1/2}$ – $^2D_{5/2}$ electric quadrupole transition of Ca^+ ions in a small radio-frequency trap. We have theoretically confirmed that an uncertainty of <1 x 10^{-15} is attainable in measurement of the $^2S_{1/2}$ – $^2D_{5/2}$ transition frequency. Experimentally, we have developed stable laser-diode systems and observed the quantum jump of single $^{40}Ca^+$ ions to the $^2D_{5/2}$ state.**

I. INTRODUCTION

The uncertainty of primary frequency standards using Cs atoms reaches around 10^{-15} and the inherent limits involved in them are discussed. On the other hand, frequency standards using new materials and methods are proposed for developing more accurate frequency standards. Recently, several groups have measured frequencies of the ionic forbidden transitions in the optical region to apply them to the clock transitions of optical frequency standards [1]. We now proceeds with study on an optical frequency standard using single Ca^+ ions. One of advantages using Ca^+ ions is that all the useful transitions are accessible with the fundamental waves of laser diodes (LDs) and we can develop a compact and reliable frequency standard [2].

Fig. 1 shows a partial term diagrams of $^{40}Ca^+$ and $^{43}Ca^+$ ions. They are laser-cooled using the $^2S_{1/2}$ – $^2P_{1/2}$ cooling transition at 397 nm and the $^2P_{1/2}$ – $^2D_{3/2}$ repumping transition at 866 nm. Lifetime of the $^2D_{5/2}$ state is ~1.2 s (natural linewidth ~0.13 Hz), which gives a very high line-Q (~10^{15}) to the quadrupole $^2S_{1/2}$ – $^2D_{5/2}$ transition at 729 nm. Laser cooling of $^{43}Ca^+$ ions requires much more complicated light sources than $^{40}Ca^+$ ions because of the hyperfine splitting of a $^{43}Ca^+$ ion and its very small natural abundance (0.14 %). An odd isotope like the $^{43}Ca^+$ ion, however, has a merit that it can avoid the very large first-order Zeeman frequency shift. Now, we are aiming to measure the $^2S_{1/2}$ – $^2D_{5/2}$ transition of $^{40}Ca^+$ ions with high accuracy using a simple laser-cooling light source system, and we are planning to apply the measurements to a development of the optical frequency standard using $^{43}Ca^+$ ions. Some theoretical estimation on the uncertainties is shown in next section. Development of the light sources and spectroscopic measurements follows that. Finally, concluding remarks and the future plan are shown.

II. FREQUENCY SHIFT ESTIMATION

In the case of even isotope like a $^{40}Ca^+$ ion, the largest source of the transition frequency uncertainty is the first-order Zeeman shift. Recently, however, a new way to reduce this uncertainty was illustrated [3] and actually demonstrated [4]. According to the measurement of the $^{88}Sr^+$ optical standard [4], whose total uncertainty was 3.4 x 10^{-15}, it would be possible to reduce the uncertainty of a $^{40}Ca^+$ ion due to the first-order Zeeman shift on the order of 10^{-15}. In the case of a $^{43}Ca^+$ ion, the first-order Zeeman shift can be avoided by measuring the quadrupole transition between its $m_F = 0$ Zeeman sub-levels. Rather, the second-order Zeeman shift and the electric quadrupole shift would be the main sources of the uncertainty. Therefore, we estimate the frequency shifts in the measurement of the $^2S_{1/2}$ – $^2D_{5/2}$ transition of a single $^{43}Ca^+$ ion.

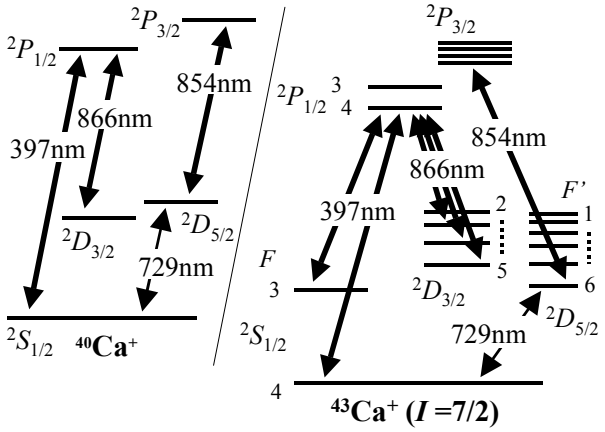

Figure 1. Partial term diagrams of of $^{40}Ca^+$ and $^{43}Ca^+$. F and F' are total angular momentum including nuclear spin I =7/2.

For a $^{43}Ca^{+}$ ion, the energy shifts ν_{hfs} of the hyperfine levels in the 4 $^2S_{1/2}$ and the 3 $^2D_{5/2}$ states are calculated as a function of J, F and I =7/2 by

$$\nu_{hfs} = \frac{A_h}{2} C + B_h \frac{3C(C+1) - 4IJ(I+1)(J+1)}{8IJ(2I-1)(2J-1)},$$
$$C = F(F+1) - I(I+1) - J(J+1)$$

and the constants A_h and B_h reported in [5] and [6], where J, I, and F are quantum numbers of total angular momentum, nuclear spin, and total angular momentum including nuclear spin, respectively. Among transitions between m_F = 0 levels, independent of the first-order Zeeman shift, transitions from the (4 $^2S_{1/2}$, F=4, m_F=0) level are useful for the measurement because of the transition selection rules at the laser cooling and the optical pumping [7]. We calculated the coefficients of the second-order Zeeman shift ν_Z for the (4 $^2S_{1/2}$, F=4, m_F=0) - (3 $^2D_{5/2}$, F'=2, 4, 6, m_F=0) transitions using

$$\nu_Z = \mu_B^2 g_J(D_{5/2})^2 B^2 \sum_{F'(\neq F)} \frac{\left|\langle D_{5/2}, F, m_F = 0 | J_z | D_{5/2}, F', m_F = 0\rangle\right|^2}{\nu(^2D_{5/2}, F) - \nu(^2D_{5/2}, F')}$$
$$- \mu_B^2 g_J(S_{1/2})^2 B^2 \frac{\left|\langle S_{1/2}, F = 4, m_F = 0 | J_z | S_{1/2}, F = 3, m_F = 0\rangle\right|^2}{\nu(^2S_{1/2}, F = 4) - \nu(^2S_{1/2}, F = 3)},$$

where μ_B is the Bohr magneton, and B is the magnetic field strength. The Lande's g-formula gives good approximations of g_J ($D_{5/2}$) = 1.2 and g_J ($S_{1/2}$) = 2.0. Table I shows that the smallest coefficient is obtained for the (4 $^2S_{1/2}$, F=4, m_F =0) - (3 $^2D_{5/2}$, F=6, m_F =0) transition.

External electric field causes the second-order Stark shift on the transition frequency. Using the oscillation strength reported in [8], the scalar polarizabilities of a Ca^+ ion in the 4 $^2S_{1/2}$ and the 3 $^2D_{5/2}$ states were calculated to be 0.011 nm^3 and 0.0035 nm^3, respectively. Therefore, the second-order Stark shift coefficient of the $^2S_{1/2}$ – $^2D_{5/2}$ transition is estimated to be ~0.6 Hz/(V/mm)^2. When an ion is trapped by a small ion trap such as used in our experiment, in which the distance between electrodes is ~1 mm and the radio-frequency (rf) voltage is lower than 500 V, the electric field near the trapped ion is estimated to be less than 0.02 V/mm. Then, the second-order Stark shift by the trapping electric field is less than 0.3 mHz. The averaged strength of the quadratic electric field of the black body radiation is calculated using the Stefan-Boltzmann law. The frequency shift caused by it is ~0.4 Hz at room temperature.

The electric quadrupole shift ν_Q of the $^2D_{5/2}$ state is estimated using

$$\nu_Q = GQ(3\cos^2\beta - 1)$$

where $G = (2e/11)\langle 3d|r^2|3d\rangle$, Q is the electric field gradient and β is the angle between the electric field gradient direction and the quantization axis of the ion [9]. We calculated $\langle 3d|r^2|3d\rangle$ and estimated that G is 0.82

TABLE I. COEFFICIENTS OF THE QUADRATIC ZEEMAN SHIFT

F of 4 $^2S_{1/2}$ levels	F' of 3 $^2D_{5/2}$ levels	Coefficient (kHz/μT^2)
4	2	-34.2
4	4	-17.2
4	6	-8.99

Hz mm^2/V. By measuring the quadrupole transition frequency for each of three mutually orthogonal orientations of a quantizing magnetic field of a constant magnitude, the electric quadrupole shift can be eliminated. As the result the uncertainty of this shift can be reduced to less than 0.1 Hz [10]. The estimations above show that the second-order Zeeman effect gives the most significant frequency shift. The uncertainty of the clock transition frequency can be expected to be less than 10^{-15} when the magnetic field is lower than 0.2 μT.

III. LIGHT SOURCES

A. Light Source System for the Laser Cooling

For the laser cooling of $^{40}Ca^{+}$ ions, we developed a light source system, which is shown in Fig. 2, consisting of an 866-nm part, a 397-nm part, a frequency-stabilized He-Ne laser (Melles Griot), and a function generator (NF). Details of this light source system are discussed in [11] and [12]. Extended cavity diode lasers (ECDLs) of the Littrow configuration are used with 866-nm (Toptica) and 397-nm (Nichia) LDs [13]. The He-Ne laser is the master laser and the ECDLs are the slave lasers. In the 866 nm part, both the laser beams from the ECDL and the He-Ne laser were coupled to a scanning transfer cavity. The cavity is made of an INVAR tube, mirrors and a piezo-transducer (PZT). Its

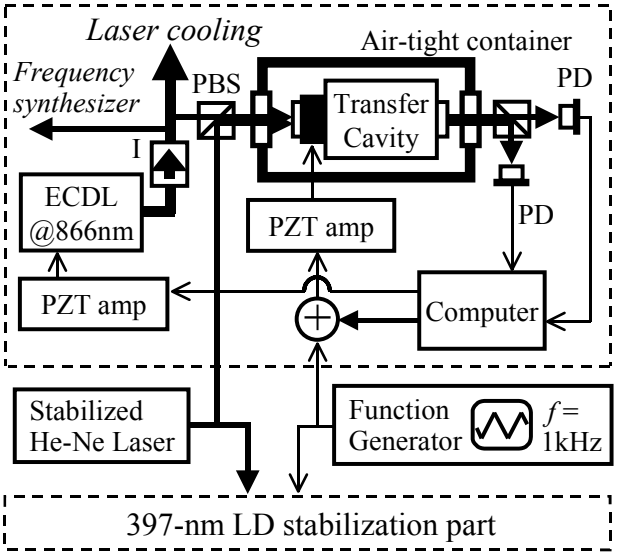

Figure 2. Light source system for the laser cooling of $^{40}Ca^{+}$ ions. ECDL: extended cavity diode laser; I: isolator; PD: photodiode; PBS: polarized-beam splitter; PZT: piezo-transducer.

free spectrum range (FSR) was 300 MHz and its finesse was ~60. The transmission of the transfer cavity was monitored by photodiodes (PD, Hamamatsu). The cavity was placed in an airtight container made of an aluminum tube and AR-coated glass windows. Temperature variance outside of the container was kept within ±0.1 K. Triangular waves of the function generator governed the cavity-length scanning. Its rate was 1 kHz and the scanning width was 5/3 FSRs (500 MHz) for the master laser. The PD signals were fed to a personal computer (PC) through a high-speed analog-digital converter (Interface).

In the first half of each triangular-wave cycle, while the cavity length increased for 0.5 ms at a fixed speed, the PC sampled the PD signals at 4 MHz. After that, the number of the PD signals sampled between the two consecutive transmission peaks of the master laser, denoted by A here, was counted. The number of PD signals between the first transmission peak of the master laser and that of the 866-nm laser, denoted by B, was also counted. The ratio $\alpha = B/A$ was compared to a constant α_0 determined by the first cavity scan. Then, the 866-nm frequency was calibrated so as to make α closer to α_0 by the proportional-integral control. The number of PD signals between the first master-laser peak and a trigger signal synchronized to each triangular wave was also kept to be constant in order to scan the transfer cavity from a fixed offset length. This procedure was repeated at a 1-kHz scanning rate. The 397 nm ECDL was stabilized in the same manner.

Some of the 866 nm light was led to an optical frequency synthesizer (Menlo Systems) to measure its frequency stability [14]. In Fig. 3, it is shown that our method improved the stability of the ECDL ~100 times better and the stability of the He-Ne laser was fully transferred to the ECDL. The frequency drift was ~300 kHz for 2 h for the stabilized ECDL. The Allan variance of 1 x 10^{-10} at 10^3 s was ~10 times better than that evaluated in the similar methods in the previous reports [15]. In this measurement, the Allan variance at an averaging time shorter than 1 s was not measured due to the limitation of the optical frequency synthesizer. The short-term end of Fig. 3, however, implies that our method is effective in the term shorter than 1 s. The frequency stability of the 397-nm ECDL could not be measured using our frequency synthesizer. Considering the effect of the variation in the air condition on the frequency stability, it was estimated that the frequency drift at 397 nm was smaller than 2 MHz per hour. These stabilities are enough for the laser cooling of Ca^+ ions because the drifts are much smaller than natural widths of the cooling and the repumping transitions. Furthermore, this stabilization scheme is applicable in the laser cooling of $^{43}Ca^+$ ions with multiple ECLDs. When we stabilize multiple ECLDs simultaneously, time sharing of one scanning transfer cavity can be utilized, in which an optical chopper selects one of the LD beams to be coupled to the transfer cavity, and the stabilization process described above is performed for the ECLDs by turns.

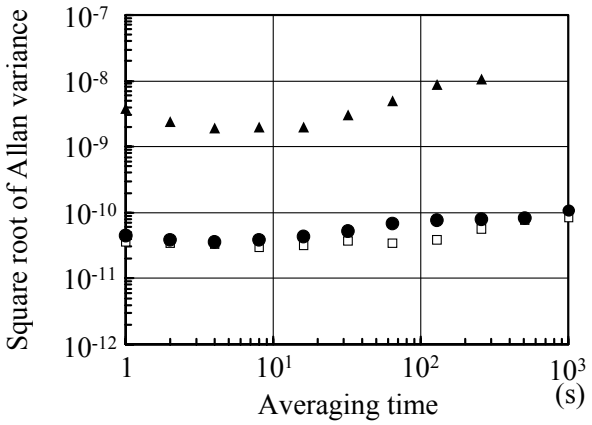

Figure 3. The Allan variance of (▲) the non-stabilized 866-nm ECDL, (●) the stabilized 866-nm ECDL, and (□) the stabilized He-Ne laser.

B. *Light Source for Quadrupole Transition Measurement*

To measure the $^2S_{1/2} - {}^2D_{5/2}$ quadrupole transition of Ca^+ ions, we have developed a highly stable frequency-tunable master-and-slave laser-diode source at 729 nm. In Fig. 4, the experimental setup is shown, and its full explanation will be given in [16]. For the master laser, an AR-coated LD (Toptica) was used in an ECDL with the Littman configuration. To compress its linewidth and frequency drift, the output of the master ECDL was coupled to a high-finesse (F = 6 x 10^4), 1-GHz-FSR ultra-low-expansion (ULE) optical cavity after it passed through an electro-optic modulator (New focus) to generate weak FM sidebands at 15 MHz and a polarization-maintaining (PM) single-mode fiber (Fujikura) to obtain a single spatial mode. The ULE cavity was put in a chamber evacuated to a pressure of 10^{-6} Pa and the chamber temperature was stabilized within ±0.01 K. The chamber was mounted on a vibration-canceling platform, and the chamber and the platform were placed in an acoustic isolation box. A Si photodiode (Hamamatsu)

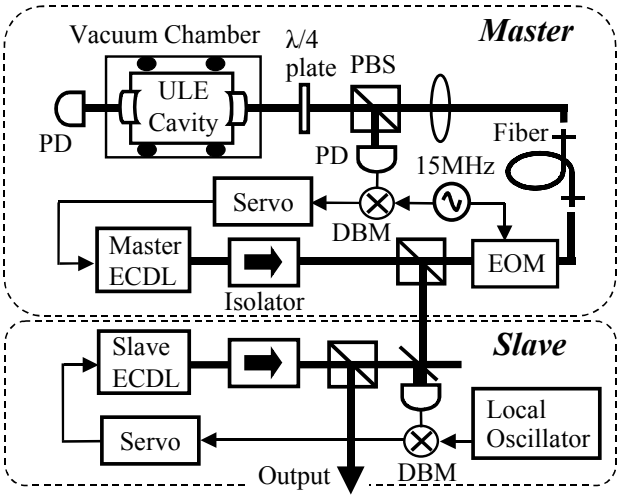

Figure 4. Light source for the quadrupole transition measurement. ULE cavity: ultra-low expansion optical cavity; DBM: double balanced mixer; EOM: electro-optic modulator.

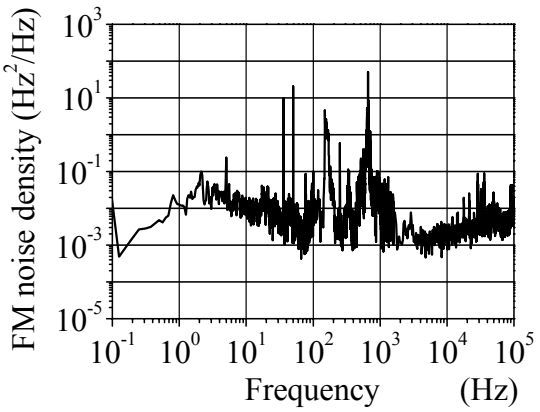

Figure 5. Power spectrum density of the stabilized master laser.

monitored the intensity of the reflected light from the ULE-cavity window. It was demodurated, integrated and fed back to the master ECDL using both a fast current feedback loop and a relatively slow PZT feedback loop [17], so that the ECDL frequency was stabilized. We measured the power spectral density of the error signal in the servo loop using a fast Fourier transform spectrum analyzer, which is shown in Fig. 5. Then, we calculated a spectrum profile of the master ECDL from the root-mean-square value of the frequency fluctuation [18], and we estimated that the full width at half maximum (FWHM) of the spectrum profile of the master ECDL was ~53 Hz relative to the ULE cavity.

Frequency tunability is indispensable for the light source to measure the quadrupole transition spectrum. For this purpose, a beatnote between a slave ECDL in the Littman configuration and the master ECDL was measured using a PD (Hamamatsu). The phase difference between the beatnote and an output of a local oscillator (ROHDE & SCHWARZ, linked to a hydrogen maser) was demodulated and processed in a phase-lock loop to lock the slave ECDL frequency to the master one with an arbitrary offset frequency [19]. We achieved an offset frequency range wider than ± 500 MHz, which covered the whole FSR of our ULE cavity (1GHz). The Allan variance of the master and the slave ECDLs was measured with the optical frequency synthesizer (Menlo system) with a microwave frequency standard linked to the International Atomic Time (TAI). The result is shown in Fig. 6. The stabilities of the master and the slave ECDLs were fully identical, and a stability of the slave ECDL of 2.2 x 10^{-13} was attained at 16-s averaging time. Because the long-term stability was limited by the thermal stability of the ULE cavity, we are improving the temperature control system.

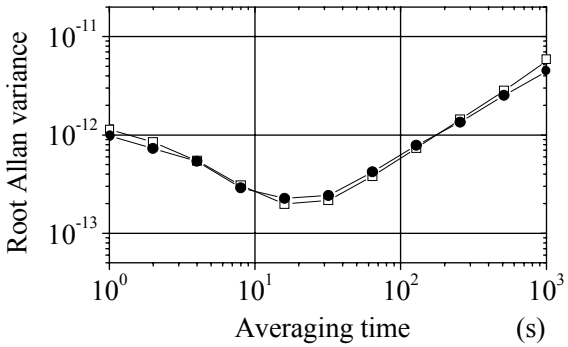

Figure 6. Allan variance of the stabilized (□) master and (●) slave lasers.

IV. SPECTROSCOPY

A. *Single $^{40}Ca^{+}$ ion trapping*

We are performing a spectroscopic study on $^{40}Ca^{+}$ ions, and now aiming to confine a single ion to a region smaller than wavelength of 729-nm light in order to eliminate the first-order Doppler broadening from the $^{2}S_{1/2} - {}^{2}D_{5/2}$ transition spectrum [20]. The experimental setup is shown in Fig. 7. A small radio-frequency trap consisting of one ring electrode and two end-cap electrodes was employed for trapping a single $^{40}Ca^{+}$ ion. The ring electrode was made of a 1.4-mm-thick 304-stainless-steel plate, which had a 1.0-mm-radius hole. The inside wall of the hole was shaped into a semicircular cross section. The end-cap electrodes were 2.0-mm-diameter rods, whose ends were shaped to be semi-spherical. The axial separation between the end-cap electrodes was 1.4 mm. Pair of auxiliary rod electrodes were placed near the end caps, and they were used to compensate the stray electric field in the trap. An rf voltage of 280 V at 18.1 MHz was applied to the ring electrode, producing a secular potential with radial and axial frequencies ω_r and

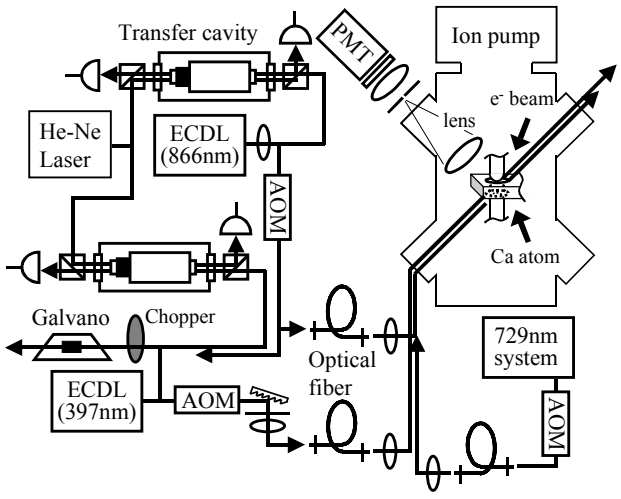

Figure 7. Experimental setup for single $^{40}Ca^{+}$ ions. AOM: acousto-optic modulator; PMT: photo-multiplier tube; Galvano: Galvano tube.

ω_z of ~2π x 0.6 MHz and ~2π x 1.3 MHz, respectively. The ion trap was put in a stainless-steel chamber evacuated to a pressure below 8 x 10^{-8} Pa. Calcium ions were created in the trap by crossing a natural Ca atomic beam and an electron beam emitted from a tungsten filament biased at –40 V.

For the laser cooling of $^{40}Ca^+$ ions, we used the light source mentioned above. Radiation at 393 nm caused the spontaneous decay to the $^2D_{5/2}$ state through the $^2S_{1/2} - {}^2P_{3/2}$ transition and it interrupted the laser cooling. Therefore, we removed the background incoherent radiation from the 397-nm ECDL output using a holographic diffraction grating [21]. The diffracted radiation at 397 nm was coupled into a PM single-mode fiber (Oz Optics) to obtain a single spatial mode. The 866-nm radiation was also coupled into a PM single-mode fiber (Fujikura). Two laser beams from the fibers were coaxially superposed, and they were focused at the center of the ion trap. The power of the 397-nm radiation at the trap center was ~80 μW and that of the 866-nm radiation was ~200 μW. The Fluorescence from the trapped $^{40}Ca^+$ ions was collected by lenses, passed through a band-pass filter at 397-nm, and detected by a photo-multiplier tube (Hamamatsu).

After the frequencies of the 397-nm and the 866-nm ECDLs were tuned to the resonance centers of $^{40}Ca^+$ ions using the optogalvano signals, the frequency of the 397-nm ECDL was set to ~100 MHz below the resonance center. We turned on the Ca oven for ~1 minute, then turned on both the oven and the tungsten filament for ~15 seconds. After turning off them, we scanned frequency of the 397-nm ECDL around the resonance of the $^{40}Ca^+$ ion, and we observed the spectrum of the laser-cooled Ca^+ ions. In Fig. 8, a single $^{40}Ca^+$ ion was laser-cooled on the low frequency side of the resonance. The maximum number of the detected photons per one $^{40}Ca^+$ ion was ~7000 /s. In Fig. 8, sudden decrease in the fluorescence intensity on the high frequency side is owing to the heating by 397-nm laser absorption. When the observed photon number was much larger than 7000 /s, multiple ions should be trapped. To make the number of the ion single, we fixed the 397-nm frequency on the high frequency side for a few tens seconds. After this procedure, the fluorescence intensity observed in the laser cooling often decreased because the heating could make some ions drop out the ion trap. Because a half width at half maximum of ~35 MHz was obtained, the FWHM was estimated to be ~70 MHz. When we neglected the power broadening and eliminated the natural linewidth of 23 MHz, the residual Doppler width of ~47 MHz was obtained using the Voigt profile. The ion temperature was estimated to be less than 0.3 K.

B. Quantum jump and quadrupole transition measurment

After observing the laser-cooling spectrum such as was shown in Fig. 8, we fixed the frequency of the 397-nm light at several MHz below the resonance and observed continuous fluorescence intensity from a single $^{40}Ca^+$ ion. The light from the slave 729-nm ECDL, as mentioned above, was coupled to a PM single-mode fiber (Fujikura), and the output from the fiber was overlapped with the cooling lasers at 397 nm and 866 nm using a dielectric mirror. Then, the 729-nm light was focused into the trap chamber with a beam waist of somewhat larger than those of the cooling lasers.

By applying the 729-nm light to a single $^{40}Ca^+$ ion, we observed the quantum jump accompanied with the $^2S_{1/2} - {}^2D_{5/2}$ transition. Typical measurements of the quantum jump are shown in Fig. 9. The gate time of the photon counting was 100 ms. The single $^{40}Ca^+$ ion was pumped into the metastable $^2D_{5/2}$ state by 729-nm light and fluorescence with the $^2S_{1/2} - {}^2P_{1/2}$ transition was fully extinguished. Fluorescence with the $^2S_{1/2} - {}^2P_{1/2}$ transition returned when the ion decayed back to the $^2S_{1/2}$ ground state.

In order to observe the spectrum line profile of the $^2S_{1/2} - {}^2D_{5/2}$ transition, we measured the rate of the quantum jump of a single $^{40}Ca^+$ ion depending on the 729-nm light frequency. The frequency of the 729-nm laser was stepped by 10 MHz and its intensity was fixed to a power of ~30 μW through the measurement. The rate was calculated from

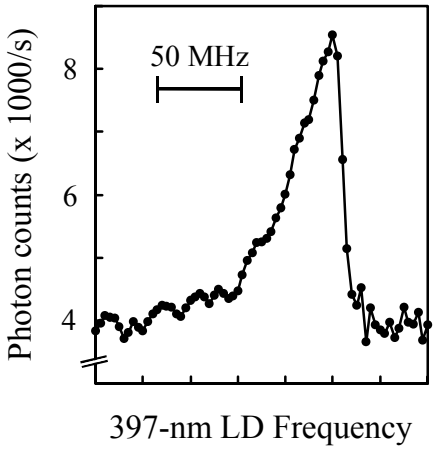

Figure 8. Spectrum of a laser-cooled single $^{40}Ca^+$ ion.

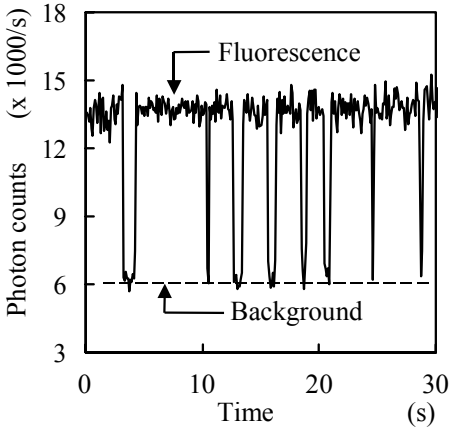

Figure 9. Quantum jumps of a single $^{40}Ca^+$ ion.

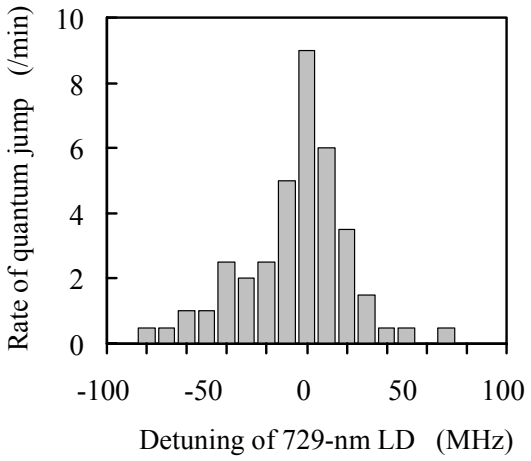

Figure 10. Histogram of the rate of the quntum jump with the 4 $^2S_{1/2}$ – 3 $^2D_{5/2}$ transition.

the number of times of the quantum jump counted for 3 minutes at each 729-nm frequency. At this 729-nm light intensity, the maximum rate of the quantum jump was lower than 10 times /min. Fig. 10 shows a histogram of the rate of the quantum jump as the function of the 729-nm frequency. Several such profiles were observed with the linewidth of the order of 25 MHz. This width seems to be suffered by the residual Doppler broadening, a combination of as many as ten unresolved Zeeman components and the power broadening caused by the 397-nm, 866-nm and 729-nm radiation. The ambient magnetic field near the ion trap was ~0.1 mT. If the measured linewidth was only due to the Doppler broadening, the ion temperature would be ~0.3 K.

To eliminate the Doppler broadening, we are improving the laser cooling using the micromotion compensation of the trapped ion. And to eliminate the power broadening caused by the 397-nm and 866-nm radiation, we are adopting a pulse sequence to our experiment, consisting of a cooling period, a quadrupole-allowed excitation period and a probing period [20]. We are planning to measure the absolute frequency of this transition using the optical frequency synthesizer.

V. CONCLUSION

Calcium ion is very attractive for application in optical frequency standards because its 4 $^2S_{1/2}$ – 3 $^2D_{5/2}$ transition, whose natural linewidth is ~0.13 Hz, is measurable with all fundamental waves of LDs. By using LD-based stable light sources and a small ion trap, we can develop a robust and compact optical frequency standard. Our theoretical estimation shows that an uncertainty of better than 1 x 10^{-15} is attainable using a single $^{43}Ca^+$ ion. For the laser cooling of Ca^+ ions, we developed a simple method stabilizing frequencies of multiple ECDLs down to the order of 100 kHz using a He-Ne laser and scanning transfer cavities. As a light source for measuring the 4 $^2S_{1/2}$ – 3 $^2D_{5/2}$ transition with a narrow linewidth, a highly stable frequency-tunable LD system at 729 nm was developed, the linewidth of which was estimated to be narrower than 60 Hz. We measured a spectrum of the 4 $^2S_{1/2}$ – 3 $^2D_{5/2}$ transition from the rate of the quantum jump of a single $^{40}Ca^+$ ion. In this measurement, the observed spectrum was limited by the residual Doppler broadening. Improvement of the laser cooling is planned.

REFERENCES

[1] S.A. Diddams, Th. Udem, J.C. Bergquist, E.A. Curtis, R.E. Drullinger, L. Hollberg, W.M. Itano, W.D. Lee, C.W. Oates, K.R. Vogel, and D.J. Wineland, "An optical clock based on a single trapped $^{199}Hg^+$ ion" Science, Vol. 293, 2001, pp. 825-828.

[2] M. Kajita, K. Matsubara, Y. Li, K. Hayasaka, and M. Hosokawa, "Preparing single ions in m = 0 states in the Lamb-Dicke regime" Jpn. J. Appl. Phys., Vol. 43, 2004, pp. 3592-3595.

[3] J. E. Bernard, L. Marmet, A. A. Madej, "A laser frequency lock referenced to a single trapped ion" Opt. Commun., Vol. 150, 1998, pp. 170-174.

[4] H. S. Margolis, G. P. Barwood, G. Huang, H. A. Klein, S. N. Lea, K. Szymaniec, and P. Gill, "Hertz-level measurement of the optical clock frequency in a single $^{88}Sr^+$ ion" Science, Vol. 306, 2004, pp. 1355-1358.

[5] W. Nortershauser, K. Blaum, K. Icker, P. Mueller, A. Schmitt, K. Wendt, and B. Wiche, "Isotope shifts and hyperfine structure in the 3d ^2D_J - 4p ^2P_J transitions in calcium II", Euro. Rhys. J. Vol. D2, 1998, pp. 33-39.

[6] D. M. Lucas, A. Ramos, J. P. Home, M. J. McDonnell, S. Nakayama, J. S. Stacey, S. C. Webster, D. N. Stacey, and A. M. Steane, "Isotope-selective photoionization for calcium ion trapping", Phys. Rev. A Vol. 69, 2004, 012711.

[7] M. Kajita, Y. Li, K. Matsubara, K. Hayasaka, and M. Hosokawa, "Prospect of the optical frequency standard based on $^{43}Ca^+$ ion", Phys. Rev. A, in press.

[8] W. L. Wiese, M. W. Smith, and B. M. Miles, Natl. Stand. Ref. Data Ser. (U. S. Natl. Bur. Stand.) Vol. 22, 1969, pp.250.

[9] W. M. Itano, "External-field shifts of the $^{199}Hg^+$ optical frequency standard ", J. of Research of N.I.S.T., Vol. 105, 2000, pp. 829-837.

[10] G. P. Barwood, H. S. Margolis, G. Huang. P. Gill, and H. A. Klein, "Measurement of the electric quadrupole moment of the 4*d* $^2D_{5/2}$ level in $^{88}Sr^+$ ", Phys. Rev. Lett. Vol. 93, 2004, 133001.

[11] K. Matsubara, S. Uetake, H. Ito, Y. Li, K. Hayasaka, and M. Hosokawa, "Precise frequency-drift measurement of extended-cavity diode laser stabilized with scanning transfer cavity" Jpn. J. Appl. Phys., Vol. 44, 2005, pp. 229-230.

[12] S. Uetake, K. Matsubara, H. Ito, K. Hayasaka, and M. Hosokawa, "Frequency stability limit of a diode laser stabilized by the scanning transfer cavity method" in press.

[13] K. Hayasaka, "Frequency stabilization of an extended-cavity violet diode laser by resonant optical feedback" Opt. Commun. Vol. 206, 2002, pp. 401-409.

[14] R. Holzwarth, M. Zimmermann, T. Udem and T. W. Hansch, "Optical clockworks and the measurement of laser frequencies with a mode-locked frequency comb", IEEE J. Quantum Electron. Vol. 37, 2001, pp. 1493-1501.

[15] A. Rossi, V. Biancalana, B. Mai and L. Tomassetti, "Long-term drift laser frequency stabilization using purely optical reference", Rev. Sci. Instrum. Vol. 73, 2002, pp. 2544-2548.

[16] Y. Li, H. Ito, K. Matsubara, M. Kajita, K. Fukuda, and M. Hosokawa, "Narrow-line and frequency tunable diode laser system for the S-D transition of Ca^+ ion" unpublished.

[17] R. W. P. Drever, J. L. Hall, F. V. Kowalski, J. Hough, G. M. Ford, A. J. Munley, H. Ward, "Laser phase and frequency stabilization using an optical-resonator", Appl. Phys. Vol. B31, 1983, pp. 97-105.

[18] Y. Shevy, J. Kitching, and A. Yariv, "Linewidth reduction and frequency stabilization of a semiconductor-laser with a combination of FM side-band locking and optical feedback", Opt. Lett. Vol. 18, 1993, pp. 1071-1073.

[19] L. Ricci, M. Meidemuller, T. Esslinger, A. Hemmerich, C. Zimmermann, V. Vuletic, W. Kenig, and T. W. Hansch, "A compact grating-stabilized diode-laser system for atomic physics ", Opt. Commun., Vol. 117, 1995, pp. 541-549.

[20] K. Toyoda, H. Naka, H. Kitamura, H. Sawamura, and S. Urabe, "Sideband-resolved spectroscopy on the 4 $^2S_{1/2}$ – $^2D_{5/2}$ transition in single calcium ions by use of fundamental waves of diode lasers" Opt. Lett., Vol. 29, 2004, pp. 1270-1272.

[21] K. Toyoda, A. Miura, S. Urabe, K. Hayasaka, and M. Watanabe, "Laser cooling of calcium ions by use of ultraviolet laser diode: significant induction of electron-shelving transitions", Opt. Lett., Vol. 26, 2001, pp. 1897-1899.